

Use of 3D MR reconstructions in the evaluation of glenoid bone loss: a clinical study

Soterios Gyftopoulos · Luis S. Beltran · Avner Yemin ·
Eric Strauss · Robert Meislin · Laith Jazrawi ·
Michael P. Recht

Received: 9 September 2013 / Revised: 26 October 2013 / Accepted: 29 October 2013 / Published online: 7 December 2013
© ISS 2013

Abstract

Objective To assess the ability of 3D MR shoulder reconstructions to accurately quantify glenoid bone loss in the clinical setting using findings at the time of arthroscopy as the gold standard.

Materials and methods Retrospective review of patients with MR shoulder studies that included 3D MR reconstructions (3D MR) produced using an axial Dixon 3D-T1W-FLASH sequence at our institution was conducted with the following inclusion criteria: history of anterior shoulder dislocation, arthroscopy (OR) performed within 6 months of the MRI, and an estimate of glenoid bone loss made in the OR using the bare-spot method. Two musculoskeletal radiologists produced estimates of bone loss along the glenoid width, measured in mm and %, on 3D MR using the best-fit circle method, which were then compared to the OR measurements.

Results There were a total of 15 patients (13 men, two women; mean age, 28, range, 19–51 years). There was no significant difference, on average, between the MRI (mean 3.4 mm/12.6 %; range, 0–30 %) and OR (mean, 12.7 %; range, 0–30 %) measurements of glenoid bone loss ($p=0.767$). A 95 % confidence interval for the mean absolute error extended from 0.45–2.21 %, implying that, when averaged over all patients, the true mean absolute error of the MRI measurements relative to the OR measurements is expected to be less than 2.21 %. Inter-reader agreement between the two readers had an IC of 0.92 and CC of 0.90 in terms of percentage of bone loss.

Conclusions 3D MR reconstructions of the shoulder can be used to accurately measure glenoid bone loss.

Keywords Glenoid bone loss · 3D MR · Anterior shoulder instability

S. Gyftopoulos (✉) · L. S. Beltran · A. Yemin · M. P. Recht
Department of Radiology, NYU Langone Medical Center, 660 First
Avenue, New York, NY 10016, USA
e-mail: soterios20@gmail.com

L. S. Beltran
e-mail: luis.beltran@nyumc.org

A. Yemin
e-mail: avneryemin@gmail.com

M. P. Recht
e-mail: michael.recht@nyumc.org

E. Strauss · R. Meislin · L. Jazrawi
Department of Orthopaedic Surgery, NYU Langone Medical Center,
Center for Musculoskeletal Care, 333 E. 38th street, New York,
NY 10016, USA

E. Strauss
e-mail: eric.strauss@nyumc.org

R. Meislin
e-mail: robert.meislin@nyumc.org

L. Jazrawi
e-mail: laith.jazrawi@nyumc.org

Introduction

The degree of anterior glenoid bone loss plays an important role in the management of patients with a history of shoulder instability as it can predispose to recurrent dislocation, even in the setting of prior capsulolabral repair [1–9]. Studies have demonstrated rates of recurrent shoulder instability between 50 and 75 % in patients who have had prior arthroscopic Bankart repair and anteroinferior glenoid bone loss greater than 25 % [2, 6, 7].

Preoperative imaging is crucial to the evaluation of this type of osseous injury with both CT and MR imaging having been shown to accurately quantify the amount of bone loss present [10–23]. Three-dimensional computed tomography (3D CT) of the shoulder is the current imaging gold standard allowing for more accurate representation and improved conceptualization of the complex glenoid anatomy, which further assists surgical planning [12, 16, 24].

Recently, 3D MR reconstructions of the shoulder have been shown to be an effective tool in the measurement of glenoid bone loss that can be acquired and post-processed in a reasonable amount of time [21]. In that cadaveric study, the estimates of bone loss using the 3D MR reconstructions were nearly identical to those obtained on 3D CT. The purpose of the current investigation is to assess the ability of 3D MR shoulder reconstructions to accurately quantify glenoid bone loss in the clinical setting using findings at the time of arthroscopy as the gold standard. We hypothesize that the 3D MR reconstructions can be used to accurately estimate glenoid bone loss.

Materials and methods

Institutional review board approval was obtained, and informed consent was waived for the retrospective Health Insurance Portability and Accountability Act-compliant study.

A retrospective review of patients who underwent MR shoulder examinations (both MR arthrograms and non-arthrographic MRIs were included) with the axial Dixon 3D-T1W-FLASH sequence included in the protocol and post-processed into 3D reconstructions at our institution over a 15-month period was conducted with the following inclusion criteria: (1) history of anterior shoulder dislocation; (2) arthroscopy (OR) performed within the 6 months after the MRI, and (3) an estimate of glenoid bone loss made in the OR using the bare-spot method. Exclusion criteria consisted of no history of prior anterior shoulder instability, surgery was not performed within the 6 months after the MRI, and no estimate of glenoid bone loss in the OR.

MRI technique

The non-arthrographic studies were performed on either a 1.5-T or 3-T MR scanner (Siemens Medical) with the following sequences: oblique coronal turbo spin echo (TSE) proton density (3 mm, TR range/TE range, 2,100–2,500/25–35) and fat-suppressed T2W (3 mm, TR range/TE range 3,500–4,000/55–60), oblique sagittal T1W (3 mm, TR range/TE range 450–600/12–15) and fat-suppressed T2W (3 mm, TR range/TE range, 3,500–4,000/55–65), and axial fat-suppressed proton density (3 mm, TR range/TE range, 2,100–2,500/25–37). For the MR arthrographic studies (performed on the same 1.5-T or 3-T MR scanners), fat-suppressed T1W axial (3 mm, TR range/TE range, 400–800/12–24), fat-suppressed T1W oblique coronal (3 mm, TR range/TE range 400–800/12–24), and fat-suppressed T1W abducted externally rotated (4 mm, TR range/TE range 450–600/12–24) sequences made up the protocol in addition to the oblique coronal fat-suppressed T2W and oblique sagittal T1W sequences described above. The field of view was 140 mm, and the matrix

was 256×256 for all the studies. The protocol also included an axial 3D dual echo-time T1-weighted FLASH sequence with Dixon-based water–fat separation with the following parameters: TR 10, TE 2.45/3.7, field of view of 200 mm, acquired voxel size 1.0×1.0×1.4 mm, reconstructed voxel size 1.0×1.0×1.0 mm, flip angle 9 deg, matrix 192×192, bandwidth of 400 Hz/pixel, number of partitions=120 and a slice thickness of 1 mm. Dedicated 16-channel shoulder array coils were used for imaging.

3D Post-processing

The water-only source images from the Dixon sequence were post-processed using standard subtraction software on a syngo MMWP workstation (VB 3oE, Siemens). The lowest mean signal intensity (water_min) from multiple ROIs placed on the soft tissues surrounding the osseous structures was used as a constant to calculate a subtraction image where the pixel values are subtracted from this constant (water_min – SI (i) with negative values being set to zero). This resulted in images with increased signal in the osseous structures, surrounded by signal poor/void soft tissue structures (Fig. 1). These subtracted Dixon images then underwent manual segmentation, generating 3D reconstructions of each shoulder (Tera Recon software (4.4.5.36.2068)) (Fig. 2).

Imaging evaluation/arthroscopy

Two musculoskeletal radiologists (4 years of experience each) blindly and independently estimated the amount of glenoid bone loss in terms of size (mm) and percentage of bone loss along the width of the glenoid on the 3D MR reconstructions using the best-fit circle method (Fig. 3). The best-fit circle



Fig. 1 A subtracted Dixon axial image of the right shoulder demonstrates the signal-rich humerus and glenoid surrounded by signal-poor soft tissue structures. An osseous Bankart fracture is seen along the anterior glenoid margin (blue arrow)



Fig. 2 A 32-year-old man with a history of recurrent shoulder instability. 3D MR reconstructions of the humeral head and glenoid are demonstrated as well as an osseous Bankart fragment (arrow)

method consists of the following parts: 1) on the sagittal (en face) view of the glenoid, a best-fit circle is drawn along the inferior aspect of the glenoid with its borders along the intact posterior and inferior margins of the glenoid, 2) a horizontal line is drawn through the center of the circle, representing an estimate of the width of an intact glenoid, 3) an additional line is drawn between the anterior margin of the circle and anterior margin of the remnant glenoid, representing the amount of bone loss, 4) this measurement is then divided by the estimate of the intact glenoid (step 2) and multiplied by 100 to generate a percentage of bone loss (25).

The arthroscopic surgeries were conducted by one of four orthopedic surgeons at our institution. The percentage of glenoid bone loss was calculated using the bare-spot method.

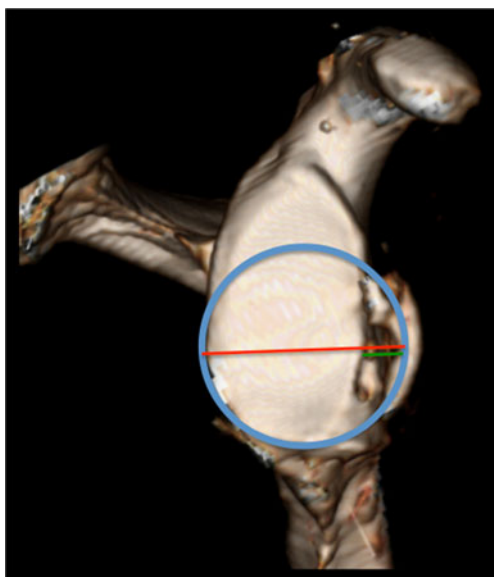


Fig. 3 The amount of glenoid bone loss is quantified using the best-fit circle method (same patient as in Fig. 2). Both MR and OR measurements estimated 20 % bone loss along the anterior aspect of the glenoid

Statistical analysis

Statistical analysis included a Wilcoxon test, Bland–Altman analysis, and 95 % confidence intervals to calculate the mean bias and absolute error for MRI in terms of the estimates of glenoid bone loss compared to the OR estimates. Inter-reader agreement was assessed using intraclass (IC) and concordance correlation (CC) coefficient analysis.

Results

A total of 57 patients had MR studies with 3D reconstructions reformatted from the axial Dixon sequences. Forty-two patients were excluded, six because no specific degree of glenoid bone loss was reported in the OR report, and 36 because they were not scheduled for surgery or had not gone to surgery by the time our study was completed. A total of 15 patients (13 men, two women; mean age, 28, range, 19–51 years) were included in the study. Two patients had MR arthrograms prior to surgery, while the other 13 had non-arthrographic MR studies. Four of the patients had prior shoulder surgery, three with prior repair of the anterior labrum and one with repair of the anterior labrum and anterior capsulorrhaphy. The mean size of the glenoid defects estimated on the 3D MR reconstructions was 3.4 mm (range, 0–8.7 mm), while the mean percentage bone loss along the glenoid width was 12.6 % (range, 0–30 %). The mean percentage bone loss along the glenoid measured during surgery was 12.7 % (range, 0–30 %). There was no significant difference, on average, between the MRI and OR measurements ($p=0.767$). A 95 % confidence interval for the mean bias extended from -1.30 to 1.03 %, implying that when averaged over all patients, the true mean difference between MRI and corresponding OR measurements is expected to be less than 1.3 %. A 95 % confidence interval for the mean absolute error extended from 0.45 to 2.21 %, implying that when averaged over all patients, the true mean absolute error of the MRI measurements relative to the OR measurements is expected to be less than 2.21 %. According to a Bland–Altman analysis to assess agreement between the measurements from MRI and OR, the 95 % limits of agreement extend from -4.2 to 4.0 %. This implies that for any one patient there is 95 % confidence that the difference between the MRI and OR measures derived for that patient will be less than 4.2 % in magnitude. For inter-reader agreement, the measurements between the two readers had an IC of 0.92 and CC of 0.90 in terms of percentage of bone loss and an IC of 0.85 and CC of 0.82 in terms of size (mm), suggesting strong agreement.

The imaging acquisition time for the Dixon sequence, which provided the raw data for the 3D reconstructions, was 3 min and 28 s. The post-processing time in the subtraction portion, done by our MR technologists, was approximately 1 min per shoulder study. The post-processing time in the

manual segmentation portion of the reconstruction, completed by our 3D lab technologists, was on average between 4 and 5 min per shoulder. The total post-processing time for each shoulder 3D MR model averaged approximately 10 min.

Discussion

Imaging plays an important role in the work-up of the patient with a history of anterior shoulder instability, especially if there is suspicion for glenoid bone loss. The presence of a defect along the anterior glenoid margin has been seen in up to 22 % of patients after their first episode of shoulder instability, and 90 % of patients with multiple episodes of shoulder instability [25, 26]. The importance of the glenoid bone loss lies in the fact that it can predispose to recurrent episodes of shoulder dislocation in both patients without prior surgery as well those who have undergone prior capsulolabral repair [1, 2, 4, 6]. An 89 % recurrence rate of shoulder instability was found by Burkhart in patients who had between 25 and 27 % glenoid bone loss [2, 4]. Tauber found glenoid rim defects in 50 % of patients who needed revision surgery for recurrent dislocation [7].

A glenoid defect increases the likelihood of shoulder instability by decreasing both the concavity compression and buttressing that help maintain contact between the glenoid and humeral head [2, 27]. This defect can also increase the shear stress on the adjacent anterior capsulolabral structures and any type of surgical stabilization, increasing the risk for failure and instability [2, 27]. The threshold for the amount of glenoid bone loss that is thought to destabilize the glenohumeral joint has varied with a range between 20 and 30 % found in both clinical and cadaveric studies [1–4, 6, 9, 16].

This threshold is one of the important factors, along with past clinical history, physical examination findings, and activity level, that the surgeon considers when deciding between treating their patient with a capsulolabral repair or osseous augmentation procedure such as with iliac bone graft or Laterjet/Bristow procedures [16, 28–32].

The arthroscopic bare spot method is a well-established technique for estimating glenoid bone loss that has been validated in several clinical and cadaveric studies, and remains the overall gold standard at our institution [4, 5, 33]. Based on the premise that the bare spot (i.e., focal thinning of cartilage along the glenoid) is located equidistant from the anterior, posterior, and inferior margins of the inferior glenoid, it can be used as a reference point to compare the posterior radius of the glenoid (which is typically intact in anterior shoulder instability patients) to the radius of the anterior glenoid; the difference of which represents the amount of bone loss.

3D CT has been the first-line imaging modality for the evaluation of glenoid bone loss for several reasons [12, 16, 23]. The anatomy of the intact glenoid is rather complex and most accurately represented by 3D CT [12, 16, 24]. 3D CT has

also been found to best and most consistently represent the extent and magnitude of injury along the glenoid margins when compared to 2D CT and MRI [16, 23]. MR imaging has been the gold standard for the evaluation of the soft tissue injuries, such as tears of the labrum and capsule, commonly seen in the setting of instability [34–38]. While several studies have suggested that MRI could be used for the characterization of glenoid bone loss, none have found it superior to 3D CT as 2D imaging like MRI has been found to misrepresent the anatomy and injuries of the glenoid when compared to 3D imaging [16, 18–20, 22, 24].

Our goal for the current study was to see if we could produce 3D reconstructions of the shoulder using MR data that would accurately reflect the glenoid anatomy and characterize the glenoid bone loss in patients with a history of prior shoulder instability. The accuracy of 3D MR reconstructions in the evaluation of glenoid bone loss was previously established in a recent cadaveric study [21]. Our study reinforces these results, demonstrating no significant difference when comparing the MR estimates to those obtained during arthroscopy ($p=0.767$), and a true mean absolute error expected to be less than 2.21 % when comparing the MR and OR measurements. There was no difference in the quality of the 3D reconstructions when comparing MR arthrographic studies and non-arthrographic MR studies.

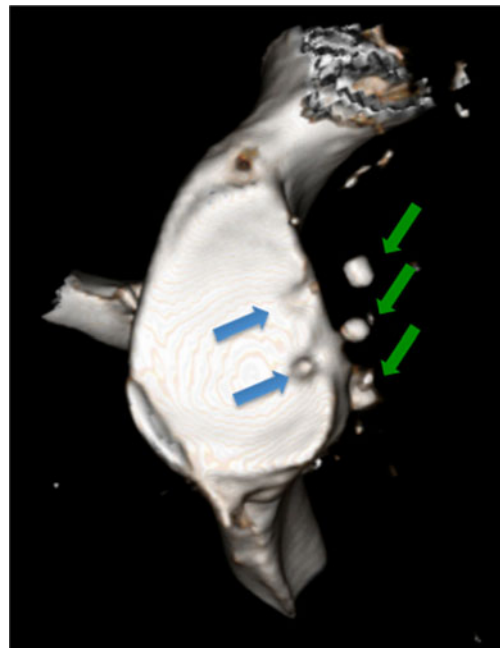


Fig. 4 A 21-year-old male with a history of prior Bankart repair and a recent episode of anterior shoulder instability. 3D MR reconstruction of the glenoid demonstrates no significant bone loss (0 % using the best-fit circle method), which was confirmed during arthroscopy (0 % using the bare spot method). The anchor tracks from the prior labral repair are demonstrated along the anterior margin of the glenoid (*blue arrows*) without distortion of the osseous anatomy. Small foci of artifact related to the prior surgery are also seen anteriorly (*green arrows*)

Use of the water-based series from the 3D FLASH-based Dixon sequence and subtraction method proved advantageous for segmentation and production of the 3D models in two ways. First, the surrounding soft tissues had all/nearly all their signal removed during subtraction resulting in areas of signal void surrounding the humerus and glenoid. Second, the subtraction indirectly resulted in not only persistent, but increased signal in the cortices and intramedullary cavities of the bones. When this data was transferred into the 3D software platform (Tera Recon), the bones were easily separated from the surrounding soft tissues. The increased signal in the humerus and glenoid resulted in “solid-appearing” 3D reconstructions and not just bone outlines. We were unable to achieve a similar degree of bone-soft tissue differentiation or a similar consolidated appearance of the 3D models when using other types of 3D acquisition sequences.

The acquisition and post-processing of MR data into 3D reconstructions in a reasonable time were important to the success of this process. The total post-processing time for each shoulder 3D MR model averaged approximately 10 min, a time similar to what it has taken our 3D laboratory to produce 3D CT reconstructions of the shoulder in the past. This time interval has allowed us to incorporate 3D MR reconstructions into our daily workflow seamlessly without delaying our final reports. The use of 3D MR reconstructions decreases the need for ordering an additional 3D CT examination for patients with suspected significant glenoid bone loss. This would spare the patient from having to undergo an additional CT study, the cost of this study, as well as the associated radiation dose.

Our study has several limitations including its retrospective nature and the small number of patients, which could predispose to a type II or beta error. A potential limitation to 3D MR may be its use in the postoperative patient, such as in the setting of prior labral repair. The suture anchors and any surrounding hardware can result in artifact, which can get magnified on certain imaging sequences like gradient echo, of which the Dixon sequence is an example. In our experience with 3D MR shoulder studies of patients with prior surgery, our results have been mixed. In some cases (like the studies in our patient population), the glenoid margins can be visualized and evaluated clearly (Fig. 4). In other cases, the artifacts related to the prior surgery make it more difficult to evaluate the anterior glenoid and quantify the bone loss. The use of the arthroscopic bare spot method may be an additional limitation. Its accuracy has been questioned as studies have found that the bare spot is not always found in the center of the glenoid [39]. In addition, the bare spot may not be present in all glenoids [17].

Conclusions

We have shown that measurements of glenoid bone loss performed on 3D MR reconstructions of the shoulder

compared favorably with the arthroscopic assessments of anterior glenoid bone loss. 3D MR reconstructions may add valuable information to what is already provided by conventional MR imaging.

Conflict of interest The authors declare that they have no conflicts of interest.

References

- Itoi E, Lee SB, Berglund LJ, Berge LL, An KN. The effect of a glenoid defect on anteroinferior stability of the shoulder after Bankart repair: a cadaveric study. *J Bone Joint Surg Am.* 2000;82:35–46.
- Burkhart SS, De Beer JF. Traumatic glenohumeral bone defects and their relationship to failure of arthroscopic Bankart repairs: significance of the inverted-pear glenoid and the humeral engaging Hill–Sachs lesion. *Arthroscopy.* 2000;16:677–94.
- Greis PE, Scuderi MG, Mohr A, Bachus KN, Burks RT. Glenohumeral articular contact areas and pressures following labral and osseous injury to the anteroinferior quadrant of the glenoid. *J Shoulder Elb Surg.* 2002;11:442–51.
- Lo IK, Perten PM, Burkhart SS. The inverted pear glenoid: an indicator of significant glenoid bone loss. *Arthroscopy.* 2004;20:169–74.
- Burkhart SS, Debeer JF, Tehrany AM, Parten PM. Quantifying glenoid bone loss arthroscopically in shoulder instability. *Arthroscopy.* 2002;18:488–91.
- Boileau P, Villalba M, Hery JY, Balg F, Ahrens P, Neyton L. Risk factors for recurrence of shoulder instability after arthroscopic Bankart repair. *J Bone Joint Surg Am.* 2006;88:1755–63.
- Tauber M, Resch H, Forstner R, Raffl M, Schauer J. Reasons for failure after surgical repair of anterior shoulder instability. *J Shoulder Elb Surg.* 2004;13:279–85.
- Bigliani LU, Newton PM, Steinmann SP, Conner PM, McIlveen SJ. Glenoid rim lesions associated with recurrent anterior dislocation of the shoulder. *Am J Sports Med.* 1998;26:41–5.
- Lynch JR, Clinton JM, Dewing CB, Warme WJ, Matsen 3rd FA. Treatment of osseous defects associated with anterior shoulder instability. *J Shoulder Elb Surg.* 2009;18:317–28.
- Stevens KJ, Preston BJ, Wallace WA, Kerslake RW. CT imaging and three-dimensional reconstructions of shoulders with anterior glenohumeral instability. *Clin Anat.* 1999;12:326–36.
- Itoi E, Lee SB, Amrami KK, Wenger DE, An KN. Quantitative assessment of classic anteroinferior bone Bankart lesions by radiography and computed tomography. *Am J Sports Med.* 2003;31:112–8.
- Kwon YW, Powell KA, Yum JK, Brems JJ, Iannotti JP. Use of three-dimensional computed tomography for the analysis of the glenoid anatomy. *J Shoulder Elb Surg.* 2005;14:85–90.
- Griffith JF, Yung PS, Antonio GE, Tsang PH, Ahuja AT, Chan KM. CT compared with arthroscopy in quantifying glenoid bone loss. *AJR.* 2007;189:1490–3.
- Chuang TY, Adams CR, Burkhart SS. Use of preoperative three-dimensional computed tomography to quantify glenoid bone loss in shoulder instability. *Arthroscopy.* 2008;24:376–82.
- Griffith JF, Antonio GE, Yung PS, Wong EM, Yu AB, Ahuja AT, et al. Prevalence, pattern, and spectrum of glenoid bone loss in anterior shoulder dislocation: CT analysis of 218 patients. *AJR.* 2008;190:1247–54.
- Provencher MT, Bhatia S, Ghodadra NS, Grumet RC, Bach BR, Dewing CB, et al. Recurrent shoulder instability: current concepts for evaluation and management of glenoid bone loss. *J Bone Joint Surg Am.* 2010;92 Suppl 2:133–51.

17. Huijsmans PE, Haen PS, Kidd M, Wouter JD, Willems JW. The shape of the inferior part of the glenoid: a cadaveric study. *J Should Elb Surg.* 2006;15:759–63.
18. Huijsmans PE, Haen PS, Kidd M, Dhert WJ, van der Hulst VP, Willems WJ. Quantification of a glenoid defect with three-dimensional computed tomography and magnetic resonance imaging: a cadaveric study. *J Should Elb Surg.* 2007;16:803–9.
19. Gyftopoulos S, Hasan S, Bencardino J, Mayo J, Nayyar S, Babb J, et al. Diagnostic accuracy of MRI in the measurement of glenoid bone loss. *AJR.* 2012;199:873–8.
20. Tian CY, Shang Y, Zheng ZZ. Glenoid bone lesions: comparison between 3D VIBE images in MR arthrography and nonarthrographic MSCT. *J Magn Reson Imaging.* 2012;36:231–6.
21. Gyftopoulos S, Yemin A, Mulholland T, Bloom M, Storey P, Geppert C, et al. 3DMR osseous reconstructions of the shoulder using a gradient-echo based two-point Dixon reconstruction: a feasibility study. *Skeletal Radiol.* 2013;42:347–52.
22. Lee RKL, Griffith J, Tong MMP, Sharma N, Yung P. Glenoid bone loss: assessment with MR imaging. *Radiology.* 2013;267:496–502.
23. Rerko MA, Pan X, Donaldson C, Jones GL, Bishop JY. Comparison of various imaging techniques to quantify glenoid bone loss in shoulder instability. *J Should Elb Surg.* 2013;22:528–34.
24. Bokor DJ, O'Sullivan MD, Hazan GJ. Variability of measurement of glenoid version on computed tomography scan. *J Should Elb Surg.* 1999;8:595–8.
25. Sugaya H, Moriishi J, Dohi M, Kon Y, Tsuchiya A. Glenoid rim morphology in recurrent anterior glenohumeral instability. *J Bone Joint Surg Am.* 2003;85:878–84.
26. Taylor DC, Arciero RA. Pathologic changes associated with shoulder dislocations: arthroscopic and physical examination findings in first-time, traumatic anterior dislocations. *Am J Sports Med.* 1997;25:306–11.
27. Lazarus MD, Sidles JA, Harryman II DT, Matsen III FA. Effect of a chondral-labral defect on glenoid concavity and glenohumeral stability: a cadaveric model. *J Bone Joint Surg Am.* 1996;78:94–102.
28. Piasecki DP, Verma NN, Romeo AA, Levine WN, Bach Jr BR, Provencher MT. Glenoid bone deficiency in recurrent anterior shoulder instability: diagnosis and management. *J Am Acad Orthop Surg.* 2009;17:482–93.
29. Latarjet M. Treatment of recurrent dislocation of the shoulder. *Lyon Chir.* 1954;49:994–7. French.
30. Helfet AJ. Coracoid transplantation for recurring dislocation of the shoulder. *J Bone Joint Surg Br.* 1958;40:198–202.
31. Warner JJ, Gill TJ, O'hollerhan JD, Pathare N, Millett PJ. Anatomical glenoid reconstruction for recurrent anterior glenohumeral instability with glenoid deficiency using an autogenous tricortical iliac crest bone graft. *Am J Sports Med.* 2006;34:205–12.
32. Provencher MT, Ghodadra N, LeClere L, Solomon DJ, Romeo AA. Anatomic osteochondral glenoid reconstruction for recurrent glenohumeral instability with glenoid deficiency using a distal tibia allograft. *Arthroscopy.* 2009;25:446–52.
33. Provencher MT, Detterline AJ, Ghodadra N, Romeo AA, Bach BR, Cole BJ, et al. Measurement of glenoid bone loss: a comparison of measurement error between 45° and 0° bone loss models and with different posterior arthroscopy portal locations. *Am J Sports Med.* 2008;36:1132–8.
34. Palmer WE, Brown JH, Rosenthal DI. Labral-ligamentous complex of the shoulder: evaluation with MR arthrography. *Radiology.* 1994;190:645–51.
35. Gusmer PB, Potter HG, Schatz JA, Wickiewicz TL, Altchek DW, O'Brien SJ, et al. Labral injuries: accuracy of detection with unenhanced MR imaging of the shoulder. *Radiology.* 1996;200:519–24.
36. Beltran J, Bencardino J, Mellado J, Rosenberg ZS, Irish RD. MR arthrography of the shoulder: variants and pitfalls. *Radiographics.* 1997;17:1403–12.
37. Zanetti M, Weishaupt D, Jost B, Gerber C, Hodler J. MR imaging for traumatic tears of the rotator cuff: high prevalence of greater tuberosity fractures and subscapularis tendon tears. *AJR.* 1999;172:463–7.
38. Hayes ML, Collins MS, Morgan JA, Wenger DE, Dahm DL. Efficacy of diagnostic magnetic resonance imaging for articular cartilage lesions of the glenohumeral joint in patients with instability. *Skeletal Radiol.* 2010;39:1199–204.
39. Kralinger F, Aigner F, Longato S, Rieger M, Wambacher M. Is the bare spot a consistent landmark for shoulder arthroscopy? A study of 20 embalmed glenoids with 3-dimensional computed tomographic reconstruction. *Arthroscopy.* 2006;22:428–32.